 doi:10.20944/preprints202206.0262.v1

Pneumatic Shape and Drag Scaling Laws of the Dandelion

Bo-Hua Sun*[1] and Xiao-Lin Guo[2]

[1]*School of Civil Engineering & Institute of Mechanics and Technology*
[2]*School of Sciences & Institute of Mechanics and Technology*
Xian University of Architecture and Technology, Xian 710055, China
**Corresponding author: B.H.S. email: sunbohua@xauat.edu.cn*

The common dandelion uses a bundle of drag-enhancing bristles (the pappus) that enables seed dispersal over formidable distances; however, the scaling laws of pneumatic/aerodynamic drag underpinning pappus-mediated flight remains unresolved. In this paper, we will study the pneumatic/aerodynamic shape of dandelion and the scaling law of resistance, and find that the drag resistance coefficient is proportional to the -2/3 power of the dandelion pappus Reynolds number. As a by-product, the terminal velocity analytical expression of the dandelion seed is also obtained.

Keywords: Dandelion, pappus, flexible filament, wind-dispersal, aerodynamic shape, drag, Reynolds number, scaling laws

The seeds of plants on Earth, such as dandelion, leave the mother and fly with the wind during the ripening season, and it is a very interesting phenomenon that plants use natural wind to spread seeds. After hundreds of millions of years of natural evolution, different seeds have evolved various but unique structures and thus have their own drag-enhancing pneumatic/aerodynamic behaviors. In order for seeds to spread over long distances, their structure is generally a disc structure composed of flexible filaments. During the process of seed flight, due to the action of hydrodynamic pressure, the flexible filament will deform to form an aerodynamic shape, thereby reducing the flow resistance [1–8].

The common dandelion uses a bundle of drag-enhancing bristles (the pappus) that helps to keep their seeds aloft (as shown in Fig.1). This passive flight mechanism is highly effective, enabling seed dispersal over formidable distances and decreasing its terminal velocity; however, the physics underpinning pappus mediated flight had not been understood until the discovery of the separated vortex ring attached to the pappus [1].

FIG. 1: Dandelion wind dispersal.

Inspired by the amazing aerodynamics features of the dandelion, very recently, Lyer et al.[8] demonstrated wind-dispersal of battery-free wireless sensing devices.

Whether it is the experimental study of Cummins, et al.[1], or the sensing devices development of Lyer et al.[8], it is necessary to understand the pneumatic/aerodynamic shape and resistance behavior of dandelion structures. Regarding the aerodynamic resistance of dandelion, their study only gave experimental scatter plots of resistance versus Reynolds numbers, and did not obtain a universal scale law; As for the pneumatic/aerodynamic shape of the dandelion, as far as the author knows, there have been no relevant theoretical and experimental research reports so far.

It is not difficult to understand that the resistance of dandelion is closely related to its pneumatic/aerodynamic shape. During the movement of the dandelion, its filaments are pneumatically deformed, so that the dandelion is deformed as a whole. This least resistant shape is the aerodynamic shape of a dandelion.

This article will examine the aerodynamic shape and resistance of dandelion. According to the structural characteristics of dandelion, assuming that all filaments are the same, the elastic deformation of each filament is first studied. To simplify, the filament is seen as a free elastic cantilever beam with a fixed bipartisan in the middle, and hydrodynamic pressure acts on the filament. In this way, the pneumatic shape of the elastic filament is obtained. We regard the overall aerodynamic resistance of the dandelion as the sum of the resistance of each filament, and obtain the relationship between the aerodynamic resistance coefficient and the dandelion Reynolds number.

Dandelion have evolved mechanisms to use wind for seed dispersal over a wide area [1–5] including creating lightweight diaspores with plumose or comose structures that act as drag-enhancing parachutes [6–8]. A bundle of flexible filaments bend in a wind in order to absorb deformation energy and reduce the drag force of the wind on the dandelion as shown in Fig.1. The flexible filaments

Preprints (www.preprints.org) | NOT PEER-REVIEWED | Posted: 20 June 2022 doi:10.20944/preprints202206.0262.v1

immersed in a flowing medium will adjust its shape to counteract flow resistance to minimizes drag by reducing, or delaying, the turbulence in boundary layer of the flow nearest the moving body.

Similar to the flexible fibre modelling in [1, 8], the dandelion pappus (a bundle of filaments) structure is regarded as a porous disk composed of many flexible filaments as shown in Fig.2.

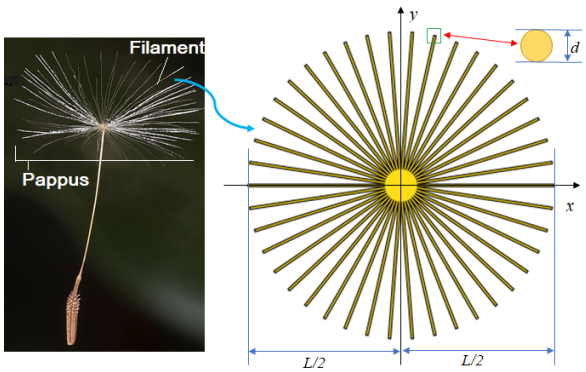

FIG. 2: The dandelion seed, structural features of the drag-generating pappus [1], beam modelling of flexible filaments.

Consider a flexible filament in the flow medium as shown in Fig.3. The filament is modelled as a thin, inextensible elastic beam loaded by the difference in fluid pressure p between its upstream and downstream sides. The flow characteristic velocity is U and no wake is considered, thus the flexible filament acted fluid pressure $[p] \approx \frac{1}{2}\rho U^2$ uniformly.

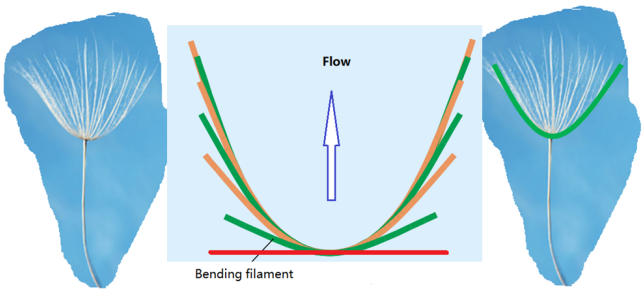

FIG. 3: The filament is supported by a thin stainless-steel rod, which is clamped at one end. Fluid drag force acting on the filament deflects this support slightly downwards.

The centerline of the beam is represented by an inextensible curve $\boldsymbol{x}(s)$ with arch length s and curvature $\kappa(s)$, Assume $\boldsymbol{x}(s)$ as a reference (middle) centerline and $\boldsymbol{n}(s)$ as the unit normal vector to the centerline of inextensible planar curve. The unit tangent of the centerline is given by $\boldsymbol{t} = \frac{d\boldsymbol{x}}{ds}$, $|\boldsymbol{t}| = 1$, which is orthogonal to the normal, ie., $\boldsymbol{t} \cdot \boldsymbol{n} = 0$. The curvature of the reference (middle) inextensible curve is $\kappa(s) = \frac{d\theta}{ds} = |\frac{d^2\boldsymbol{x}}{ds^2}| = |\frac{d\boldsymbol{t}}{ds}|$, where θ is denoted as the angle between $\boldsymbol{t}$ and horizontal axis x. The shape of the centerline can be reconstructed by relations: $\frac{dx}{ds} = \cos\theta(s)$ and $\frac{dy}{ds} = \sin\theta(s)$.

The Euler-Bernoulli beam under fluid dynamic pressure was formulated by Alben et al. [9, 10], Sun and Guo [11] and can be used to dandelion flexible filament as follows:

$$-\frac{d}{ds}(T\boldsymbol{t}) + \frac{d}{ds}(J\frac{d\kappa}{ds}\boldsymbol{n}) = d[p]\boldsymbol{n}, \tag{1}$$

where d is the diameter of the filament, T is the line tension, $J = EI$ is the bending rigidity, the Young modulus is E, area moment of inertia is I, $[p] = \frac{1}{2}\rho U^2$ is the fluid pressure jump across the filament.

At the fibre ends, there are no bending moment, transverse shear force and extensional force, so that the boundary conditions are: $T = \kappa = \frac{d\kappa}{ds} = 0$. Using planar Frenet's frame formula, namely $\frac{d\boldsymbol{t}}{ds} = \kappa\boldsymbol{n}$ and $\frac{d\boldsymbol{n}}{ds} = -\kappa\boldsymbol{t}$, Eq.1 can be decomposed into tangential and normal components: Integrating one of it with respect to arc length and applying the boundary condition, we have $T = -\frac{1}{2}J\kappa^2$. And leads to a single ordinary differential equation (ODE): $J\frac{d^2\kappa}{ds^2} + \frac{1}{2}J\kappa^3 = \frac{1}{2}\rho U^2 d$. If introducing $\bar{s} = s/L$ and $\bar{\kappa} = d\theta/d\bar{s} = L\kappa$, The ODE and corresponding boundary conditions can be noncommissioned as to the form:

$$\frac{d^2\bar{\kappa}}{d\bar{s}^2} + \frac{1}{2}\bar{\kappa}^3 = \eta^2, \quad \bar{\kappa}_{\bar{s}=\frac{1}{2}} = \left(\frac{d\bar{\kappa}}{d\bar{s}}\right)_{\bar{s}=\frac{1}{2}} = 0, \tag{2}$$

in which, the Alben number was introduced by Alben,et al. [9] as follows: $\eta = \left[\frac{\frac{1}{2}\rho U^2 dL^2}{(J/L)}\right]^{1/2}$.

The aerodynamic shape of the fibre can be reconstructed by relations: $\frac{d\bar{x}}{d\bar{s}} = \cos\theta(s)$ and $\frac{d\bar{y}}{d\bar{s}} = \sin\theta(s)$, where $\bar{x} = x/L$, $\bar{y} = y/L$, and shown in Fig.4.

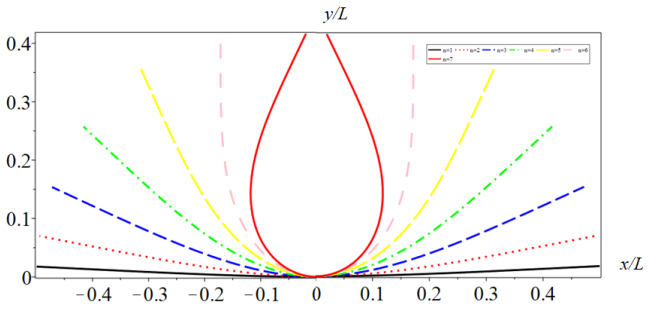

FIG. 4: The aerodynamics shape $(\bar{x}, \bar{y})$ for different parameter $\eta = 3n/2$, $n = 1, 2, 3..., 7$, the aerodynamic shape is symmetric to the y axis.

For the problem, there are 6 quantities, namely D, ρ, J, , ν, U, A, where ν is kinematic viscosity and $A = Ld$. The quantity dimensions are listed in the following table I:

Preprints (www.preprints.org) | NOT PEER-REVIEWED | Posted: 20 June 2022 doi:10.20944/preprints202206.0262.v1

TABLE I: Dimensions of physical quantities

Variables	Notation	Dimensions
Filament's Drag	D_f	MLT^{-2}
Mass density	ρ	ML^{-3}
Rigidity	J	$\mathrm{ML}^3\mathrm{T}^{-2}$
Kinematic viscosity	ν	L^2t^{-1}
Flow velocity	U	LT^{-1}
Area($= Ld$)	A	L^2

The dimensional basis used is length (L), mass (M) and time (T).

The drag D_f can be expressed as the function of quantities ρ, E, , ν, U, A, namely,

$$D_f = f(\rho,\ E, , \nu,\ U,\ A). \tag{3}$$

In the above relation, there are 6 quantities, two of them are dimensionless. Since only 3 dimensional basis L,M,T are used, so according to dimensional analysis of Buckingham [12], Eq. 3 produces 3 dimensionless quantities Π. The first one is: $\Pi_D = D\rho^a U^b A^c = L^0M^0T^0$,, we have $\Pi_{D_f} = \frac{D_f}{\frac{1}{2}\rho U^2 A}$, Similarly, for J, we have $\Pi_J = \frac{J}{\frac{1}{2}\rho U^2 A^2}$ and for ν, we have $\Pi_\nu = \frac{\nu}{\rho U\sqrt{A}}$.

From Buckingham Π theorem [12–14], the Eq.3 can be equivalency expressed as $\Pi_{D_f} = f(\Pi_J, \Pi_\nu)$, namely

$$D_f = \frac{1}{2}\rho U^2 A f(\frac{J}{\frac{1}{2}\rho U^2 A^2}, \Pi_\nu). \tag{4}$$

For single filament, its Reynolds number Π_ν can be ignored, we can propose an approximate $f(\frac{J}{\frac{1}{2}\rho U^2 A^2}, \Pi_\nu) \approx C_0\left(\frac{J}{\frac{1}{2}\rho U^2 A^2}\right)^\alpha$, therefore

$$D_f \approx C_0 \frac{1}{2}\rho U^2 A \left(\frac{J}{\frac{1}{2}\rho U^2 A^2}\right)^\alpha, \tag{5}$$

where C_0 is a constant and α is an exponent to be determined by experiments.

From Alben, Shelley and Zhang [9, 10], Sun and Guo [11], for $\eta \le 1$, we have $\alpha = 0$, for $\eta \ge 1$, we have $\alpha = \frac{1}{3}$, therefore the drag of single filament is given by

$$D_f = \begin{cases} C_1 \frac{1}{2}\rho L d U^2, & (\eta \le 1), \\ C\left[(\frac{1}{2}\rho)^2 JLd\right]^{1/3} U^{4/3}, & (\eta \ge 1). \end{cases} \tag{6}$$

where C_1, C are a constants

If the pappus of the dandelion are consist of n filaments, the total drag of the dandelion is the summation of each filament and since we assumed all filaments are the same, therefore we have the total drag of the dandelion

$$D = nD_f = \begin{cases} nC_1 \frac{1}{2}\rho L d U^2, & (\eta \le 1), \\ nC\left[(\frac{1}{2}\rho)^2 JLd\right]^{1/3} U^{4/3}, & (\eta \ge 1). \end{cases} \tag{7}$$

Thus we can get the total drag coefficients of the dandelion as follows

$$C_D = \frac{D}{\frac{1}{2}\rho U^2 nLd} = \begin{cases} C_1, & (\eta \le 1), \\ C\left[\frac{J}{\frac{1}{2}\rho U^2 (Ld)^2}\right]^{1/3}, & (\eta \ge 1). \end{cases} \tag{8}$$

in which, the case of $\eta \le 1$ is corresponding to the rigid filament. we will not going to use C_1.

With the total drag in Eq.7, if we assume the weight of total dandelion seed is mg, then we have balance relation $mg = D = nD_f$, which gives the terminal velocity U of the dandelion as follows

$$U = C_U (mg)^{1/12}, \tag{9}$$

Analytically predict the terminal velocity has not been reported, where the coefficient $C_U = 4^{1/4}(nC)^{-1/12}(\rho^2 JLd)^{-1/4}$. The terminal velocity log profile is depicted in Fig.5.

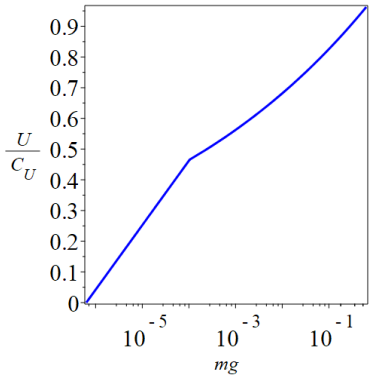

FIG. 5: Terminal velocity vs. mg.

The Reynolds number is a non-dimensional parameter characterizing the relative importance of inertial to viscous forces in a fluid. The flow through and around the pappus involves two different Reynolds numbers: that of the entire pappus ($Re = \rho UL/\mu$, in which U is the velocity of the seed, L is the diameter of the pappus and μ the dynamics viscosity of the fluid) and that of an individual filament ($Re_f = \rho Ud/\mu$). The study of Cummins et al.[1] revealed that the pappus of a dandelion benefits from a 'wall effect' at low $Re_f = \rho Ud/\mu$. Neighbouring filaments interact strongly with one another because of the thick boundary layer around each filament, which causes a considerable reduction in air flow through the pappus.

From the Reynolds numbers of the entire pappus $Re = \rho UL/\mu$, we have $U = \frac{\mu Re}{\rho L}$. Replaying the velocity U in the 2nd expression of Eq.8, we have the total drag coefficient in terms of entire pappus Reynolds number as follows

$$C_D = C\left(\frac{2\rho J}{\mu^2 d^2}\right)^{1/3} Re^{-2/3}, (\eta \ge 1). \tag{10}$$

Preprints (www.preprints.org) | NOT PEER-REVIEWED | Posted: 20 June 2022 doi:10.20944/preprints202206.0262.v1

The expression reveals that the total drag of the dandelion is proportional to $-2/3$ power law of the pappus Reynolds number, namely $C_D \sim Re^{-2/3}$.

If assume all filaments are circular solid cross-section, then the area moment of inertia I can be calculated as $I = \pi d^4/64$, inserting it to Eq.10, we have

$$C_D = C\left(\frac{\pi\rho E d^2}{32\mu^2}\right)^{1/3} Re^{-2/3}, (\eta \geq 1). \qquad (11)$$

To verify our scaling law in Eq.10, we depicted comparisons with Cummins et al. [1] and Lyer, et al. [8] in Fig. 6 and Fig.7, respectively.

With the help of our scaling law in Eq.10 and data fitting, we obtain $C_D - Re$ approximate analytical relations for Cummins et al. [1]. The solid lines are from our formula Eq.10, for blue solid line $C_D = 350Re^{-2/3}$ and for red solid line $C_D = 250Re^{-2/3}$ as shown in Fig. 6.

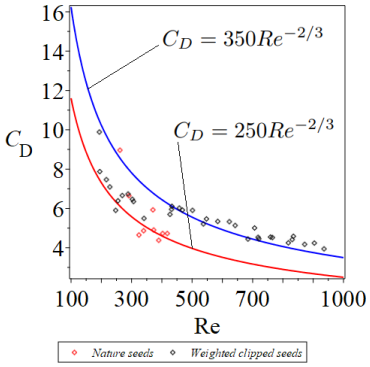

FIG. 6: Comparisons with experimental data provided Cummins et al. [1]. The drag coefficient C_D for natural (red filled circle) and artificially weighted/clipped (black filled circle) dandelion seeds as a function of Re.

In the same way, we obtain $C_D - Re$ approximate analytical relations for Lyer et al. [8]. The solid lines are from our formula Eq.10, for green solid line $C_D = 380Re^{-2/3}$, for blue solid line $C_D = 295Re^{-2/3}$ and for red solid line $C_D = 250Re^{-2/3}$ as shown in Fig.7.

Our study obtained not only the pneumatic/aerodynamic shape of the filament, but also the universal drag scaling laws of the dandelion. As a by-product, the terminal velocity analytical expression of the dandelion seed is also obtained.

To the best of the authors' knowledge, this is the first detailed study of dandelion's drag in the context of the dimensional analysis. The total drag of the dandelion is proportional to $-2/3$ power law of the pappus Reynolds number, namely $C_D \sim Re^{-2/3}$, reveals that the softer filament the smaller the drag, which is the secret of reducing drag by fine hairs [15].

For insight perspectives, due to the generality of the scale law we obtain using dimensional analysis, we can even bravely predict that the resistance coefficients of all structures with flexible filaments obey the same law as $C_D \sim Re^{-2/3}$.

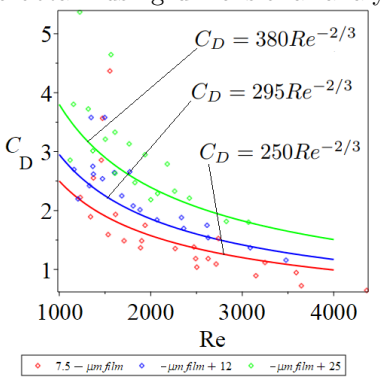

FIG. 7: Comparisons with experimental data provided Lyer et al. [8]. The drag coefficient C_D for disk with film thickness 7.5μm (red filled circle), for disk with film thickness 12μm (blue filled circle) and for disk with film thickness 25μm (green filled circle) dandelion seeds as a function of Re.

Acknowledgements

This work was supported by Xi'an University of Architecture and Technology (Grant No. 002/2040221134). The authors wish to thank Prof. Hai-Hang Cui from Xi'an University of Architecture and Technology for bringing the dandelion to our attention.

[1] Cummins, C. et al. A separated vortex ring underlies the flight of the dandelion. Nature 562, 414-418 (2018).
[2] Lentink, D., Dickson, W. B., van Leeuwen, J. L. and Dickinson, M. H. Leading-edge vorticeselevate lift of autorotating plant seeds. Science 324, 1438-1440 (2009).
[3] Greene, D. F. The role of abscission in long-distance seed dispersal by the wind. Ecology86, 3105-3110 (2005).
[4] Greene, D. F. and Johnson, E. A. The aerodynamics of plumed seeds. Funct. Ecol. 4, 117-125(1990).
[5] Vogel, S. Life in Moving Fluids: The Physical Biology of Flow 2nd edn (Princeton Univ. Press, 2020).
[6] Andersen, M. C. Diaspore morphology and seed dispersal in several wind-dispersed Asteraceae. Am. J. Bot. 80, 487 – 492 (1993).

[7] Casseau, V., De Croon, G., Izzo, D. and Pandolfi, C. Morphologic and aerodynamic considerations regarding the plumed seeds of Tragopogon pratensis and their implications for seed dispersal. PLoS ONE 10, e0125040 (2015).

[8] V. Lyer, H. Gaensbauer, T.L. Daniel and S. Gollakota, Wind dispersal of battery-free wireless devices, Nature, 603, 427-433(2022).

[9] Alben, S., Shelley, M. and Zhang, J. Drag reduction through self-similar bending of a flexible body, Nature 420, 479-481 (2002).

[10] Alben, S., Shelley, M. and Zhang, J. How flexibility induces streamlining in a two-dimensional flow, Phy. Fluids, 16(5)：1694-1713 （2004).

[11] B.H. Sun and X.L.Guo, Aerodynamic Shape and Drag Scaling Laws of Flexible Fibre in Flowing Medium. Preprints 2022, 2022050382 (doi: 10.20944/preprints202205.0382.v1).

[12] Buckingham E. On physically similar systems: illustration of the use of dimensional equations[J]. Phys. Rev. 1914, 4:345 – 376.

[13] P.W. Bridgman, *Dimensional Analysis*. Yale University Press, New Haven (1922).

[14] B.H. Sun, *Dimensional Analysis and Lie Group*, China High Education Press, Bejing (2016).

[15] S. Gao, S. Pan, H.C. Wang and X.L. Tian, Shape Deformation and Drag Variation of a Coupled Rigid-Flexible System in a Flowing Soap Film, Phy. Rev. Lett. 125, 034502 (2020).